

## MARSIS, a radar for the study of the Martian subsurface in the Mars Express mission

G. Picardi<sup>1</sup>, D. Biccari<sup>1</sup>, M. Cartacci<sup>1</sup>, A. Cicchetti<sup>1</sup>, O. Fuga<sup>1</sup>, S. Giuppi<sup>1</sup>, A. Masdea<sup>1</sup>,  
R. Noschese<sup>1</sup>, R. Seu<sup>1</sup>, C. Federico<sup>2</sup>, A. Frigeri<sup>2</sup>, P. T. Melacci<sup>3</sup>, R. Orosei<sup>4</sup>,  
O. Bombaci<sup>5</sup>, D. Calabrese<sup>5</sup>, E. Zampolini<sup>5</sup>, L. Marinangeli<sup>6</sup>, E. Pettinelli<sup>7</sup>, E. Flamini<sup>8</sup>,  
and G. Vannaroni<sup>9</sup>

<sup>1</sup> Università di Roma “La Sapienza”, Dipartimento INFOCOM, Via Eudossiana 18, I-00184 Roma, Italy

<sup>2</sup> Università di Perugia, Dipartimento di Scienze della Terra, Piazza dell’Università 1, I-06123 Perugia, Italy

<sup>3</sup> Università di Perugia, Dipartimento di Matematica e Informatica, Via Vanvitelli 1, I-06123 Perugia, Italy

<sup>4</sup> Istituto Nazionale di Astrofisica, Istituto di Astrofisica Spaziale e Fisica Cosmica, Via del Fosso del Cavaliere 100, I-00133 Roma, Italy

<sup>5</sup> Alcatel Alenia Space, Via Saccomuro 24, I-00131, Roma, Italy

<sup>6</sup> Università “D’Annunzio”, Dipartimento di Scienze, International Research School of Planetary Sciences, Viale Pindaro 42, I-65127 Pescara, Italy

<sup>7</sup> Università di Roma “Roma Tre”, Dipartimento di Fisica, Via della Vasca Navale 84, I-00146, Roma, Italy

<sup>8</sup> Agenzia Spaziale Italiana, Viale Liegi 26, I-00198 Roma, Italy

<sup>9</sup> Istituto Nazionale di Astrofisica, Istituto di Fisica dello Spazio Interplanetario, Via del Fosso del Cavaliere 100, I-00133 Roma, Italy  
e-mail: picar@infocom.uniroma1.it

**Abstract.** MARSIS (Mars Advanced Radar for Subsurface and Ionosphere Sounding) is a subsurface sounding radar on board the European Space Agency mission Mars Express. The MARSIS primary scientific objective is to map the distribution of water, both liquid and solid, in the upper portions of the crust of Mars. Detection of such reservoirs of water will address key issues in the hydrologic, geologic, climatic and possible biologic evolution of Mars. Three secondary scientific objectives are subsurface geologic probing, surface characterization and ionosphere sounding. In this paper an inversion approach of MARSIS data is presented. The data inversion (estimation of the materials composing the surface and the subsurface by the estimation of the dielectric constants) is based on the analysis of the data available from the MARSIS observations, that is the surface to subsurface power ratio and the relative time delay. The data inversion has been performed with a multi frequency analysis in order to estimate the frequency dependent parameters affecting the behavior of the radar echoes. The data inversion needs a hypothesis on the surface composition to give an geological interpretation of the subsurface dielectric properties. To improve the validity

of the obtained solutions it is necessary to introduce few constraints relevant to the geological history of the surface, to the local temperature and the thermal condition of the observed zones and the results of other instruments of Mars Express and of other missions to Mars. This approach, that is addressed to evidence the radar capabilities, is a first step for the interpretation of the results by the geologist.

**Key words.** Space vehicles: instruments – Techniques: radar astronomy – Planets and satellites: individual: Mars

## 1. Introduction

In this paper a preliminary inversion approach of MARSIS (Mars Advanced Radar for Subsurface and Ionosphere Sounding) data (Picardi et al. 2004, 2005) is presented. The data inversion procedure is based on a knowledge of the absolute value of the surface layer dielectric constant and on the measured attenuation between the first echo and the one pertaining to the interface together with the time delay between the first surface reflection and the interface. It has to be highlighted the uncertainty on the absolute value of this dielectric constant due to the difficulties on the calibration of the antenna radiation factor, on the value of the transmitted power and on the MARSIS receiver gain. The relative power measurements are more accurate and are within the accuracy specified for the radar.

The subsurface echoes signal, in sounder operative mode (MARSIS working as a pulse limited altimeter) can be hidden by synchronous echoes coming from off nadir surface reflections (surface clutter); moreover this clutter, arriving from the across track direction, can be interpreted as a signal coming from a subsurface interface. In the along track direction the clutter is filtered by the synthetic aperture antenna processing. Presently, in absence of the commissioning of the monopole antenna that contribute to the clutter cancellation, we are analyzing the return echoes from Mars regions focusing our attention on the areas where the surface can be considered flat avoiding, in this way, the risk of wrong interpretation of the echoes signals. Moreover, once detected a potential subsurface signal on the processed data at a depth  $\delta$ , in order to confirm that the interface is present, it is necessary to perform the following processing and verifications:

1. Subsurface return echoes estimation (depth, level and spatial correlation).
2. Analysis of surface within a range  $\sqrt{2} h \delta$  ( $h$  = satellite height,  $\delta$  = interface potential height) in order to avoid to confuse interface with clutter coming from the surface: source of backscattering identification by analysis of the maps of the slope  $m$  and the angles  $\alpha_x$  and  $\alpha_y$  obtained from 1/128 deg MOLA DEM (Smith et al. 2001). In addition a comparison of the real frames with the one generated by the surface echoes simulator is performed in order to validate the clutter backscattering.
3. Multi frequency analysis to obtain attenuation factor.
4. Analysis of the return echoes from the same surface, performed on the adjacent available orbits to differentiate between surface and subsurface echoes (subsurface echoes will be present the same distance from the first surface echo).
5. Multi look analysis to reduce the speckle noise.
6. Ionosphere plasma frequency estimation (by contrast loop results, surface profiles, etc.).

## 2. Reference layer models

In order to simplify the data inversion few reference models have been selected to perform easily the interpretation of the Mars surface and subsurface composition. The inverted data needs to

---

*Send offprint requests to:* G. Picardi

**Table 1.** Natural materials deemed to be present in the Martian surface and subsurface, with their dielectric properties.

Material	Percentage	$\epsilon'$	$\tan \delta$
TYPE 1	> 70% H <sub>2</sub> O ice + 30%CO <sub>2</sub> ice	2.81	0.001
TYPE 1	> 70% CO <sub>2</sub> ice + 30% H <sub>2</sub> O ice	1.87	0.0013
TYPE 2 + TYPE 3	basaltic-andesite with >70% H <sub>2</sub> O ice	4.27	0.0077
TYPE 4 + TYPE 5	basaltic-andesite with 50% H <sub>2</sub> O ice	4.79	0.012
TYPE 6 + TYPE 8	basaltic-andesite with 15% H <sub>2</sub> O ice	5.83	0.02
TYPE 7	trachy-basalt with <15% H <sub>2</sub> O ice	5.48	0.0016
TYPE 9	gypsum + halite (powder)	2.67	0.013
TYPE 10	hematite mix 10% vol., grain size 200-500 $\mu\text{m}$	3.85	0.001

be analyzed by geologists to identify the most probable association with the dielectric constant estimated by the inversion process.

According to the suggestions of planetary scientists, the reference layer models, representing the most likely detection scenario are described below.

Ice/water interface detection scenario (I/W): according to this model, the porosity of the Martian megaregolith is maximum at the surface and its decay with the increasing depth is given by an exponential law (the decay constant that can be assumed of the order of 2.8 km). The pores are filled with ice from the surface down to a depth below which liquid water is stable and becomes the pore-filling material. The change of the pore-filling material causes a discontinuity of the overall dielectric constant, which can be detected by the radar sounder.

Dry/ice interface detection (D/I): here the pore-filling material is considered to be gas or some other vacuum-equivalent material up to a depth, below which ice fills the pores. Hence the interface to detect is between dry and ice-filled materials.

Pure Ice/Crust material interface detection scenario (PI/CM): the composition of first layer of ICE (eventually with insertion of granular materials) must be taken into account.

Solid CO<sub>2</sub>/Crust material interface detection scenario (CO<sub>2</sub>/CM): Moreover the composition of first layer of CO<sub>2</sub> (eventually with insertion of granular materials) must be also taken into account.

In Table 1 are resumed few preliminary information of the first layers composition of the Mars surface.

In Table 2 are shown the value of permittivity,  $\tan \delta$  and  $\tan \delta_i$  for few materials that can be present in the surface or the subsurface of Mars.

### 3. Surface and subsurface reflectivity

According to the well known subsurface radar theory, when a short pulse of electromagnetic energy is directed toward the ground:

- The pulse reflects off an electrical boundary, and the reflected signal is received at an antenna and recorded.
- The time delay of the echo can be converted to depth: the propagation speed of the medium can be estimated
- The intensity of the reflection can be analyzed to estimate the reflectivity at the interface and the attenuation properties of the intervening layers.

**Table 2.** Other natural materials deemed to be present in the Martian surface and subsurface, with their dielectric properties.

	$\epsilon'$	$\tan \delta$	$\tan \delta_i$	
Carbonate	6.5-8	0.006	0.083-0.09	
Dense basalt (dp < 1km)	5	0.004	0.073	
Dense basalt (dp > 1km)	9	0.03	0.099	
Eolian sediment	2.4	0.03	0.056	
Fluvial sediment	1.5-8.5	0.03	0.05-0.096	0.2-0.07
Indurated sediment	2.1-2.8	0.03	0.054-0.059	
Crater ejecta	8	0.014	0.092	
Layered basalt	7.1	0.014	0.087	
Vesicular basalt	7.1	0.014	0.087	
Volcanic ash	5.6-6.5	0.013-0.04	0.077-0.083	

The surface return echoes (arriving from across track direction) can reduce the visibility of the subsurface echoes.

To assess the interface detection performance of the radar sounder it is required to evaluate the back scattering cross sections of concurrent echoes, coming from the surface and subsurface layers, given by:

$$\begin{aligned}\sigma_s &= \Gamma_s f_s(H_s, s_s, \lambda) \\ \sigma_{ss} &= \Gamma_{ss} f_{ss}(H_{ss}, s_{ss}, \lambda)\end{aligned}\quad (1)$$

being  $\Gamma_s$  and  $\Gamma_{ss}$  the Fresnel reflectivity terms, which deal with the surface and subsurface dielectric properties,  $f_s$  and  $f_{ss}$  the scattering terms, which deal with the geometric structure of the surface and subsurface (e.g. Geometric optics or Hagfors model),  $H_s$  ( $H_{ss}$ ) the Hurst exponent for the surface (subsurface), which is a parameter connected to the fractal dimension of a self-affine topography (Orosei et al. 2003),  $s_s$  ( $s_{ss}$ ) the slope for the surface (subsurface) and  $\lambda$  the wavelength.

In presence of a mixture the dielectric constants can be obtained by the Maxwell-Garnett model where  $\epsilon_i$  and  $\epsilon_h$  are respectively the dielectric constant of the intrusion and of the host material.

$$\epsilon_m(z) = \epsilon_h \frac{1 + 2 \phi(z) y}{1 - \phi(z) y} \quad (2)$$

where

$$y = \frac{\epsilon_i - \epsilon_h}{\epsilon_i + 2\epsilon_h} \quad (3)$$

and

$$\phi(z) = \phi(0) \exp\left(-\frac{z}{K}\right) \quad (4)$$

is the porosity at depth  $z$  and  $K$  is a scaling constant put at 2.8 km (Clifford 1993).

The surface Fresnel reflectivity is:

$$\Gamma_s = \left| \frac{1 - \sqrt{\varepsilon_{r1}(0)}}{1 + \sqrt{\varepsilon_{r1}(0)}} \right|^2 = R_{01}^2 = |R(0)|^2 = \alpha_{ss0} \quad (5)$$

The Fresnel reflectivity for a subsurface layer, located at a depth  $z$ , is equal to

$$\Gamma_{ss,z} = R_{12,z}^2 (1 - R_{01}^2)^2 10^{-0.1 \int_0^z \alpha(\zeta) d\zeta} \quad (6)$$

where the interface reflection coefficient is given by

$$R_{12,z}^2 = \left| \frac{\sqrt{\varepsilon_{r1}(z)} - \sqrt{\varepsilon_{r2}(z)}}{\sqrt{\varepsilon_{r1}(z)} + \sqrt{\varepsilon_{r2}(z)}} \right|^2 \quad (7)$$

In PI/CM case the term  $R_{12}^2$  is independent from the frequency and from the penetration depth.

The two way attenuation per meter is given by (Porcello et al. 1974)

$$\alpha(\zeta) = 1.8 \cdot 10^{-7} f_0 \sqrt{\varepsilon} \tan \delta \text{ dB/m} \quad (8)$$

The Subsurface to Surface power ratio of the return echo, by supposing that the surface and the subsurface interfaces have the same roughness ( $f_s = f_{ss}$ ) and neglecting the terms  $(1 - \Gamma_{ss}^2)$ , is given by:

$$\begin{aligned} P_s|_{dB} &= \Gamma_s|_{dB} + f_s|_{dB} \Rightarrow \\ P_{ss}|_{dB} &= (1 - \Gamma_s)^2|_{dB} + R_{12}^2|_{dB} + \int \alpha + f_{ss}|_{dB} \end{aligned} \quad (9)$$

Thus, if  $f_{ss}|_{dB} = f_s|_{dB}$ , then

$$\begin{aligned} \frac{P_{ss}}{P_s}|_{dB} &\approx R_{12}^2|_{dB} + \int \alpha - \Gamma_s|_{dB} \\ &= \alpha_{ss}|_{dB} \Rightarrow \frac{P_{ss,min}}{P_s}|_{dB} \Rightarrow \text{depth} \end{aligned} \quad (10)$$

In Fig. 1 are shown the graphs representing the value of  $\alpha_{ss}$  in Eq. 10, for different composition of reference layer models, expanded up to the quadratic term.

The linear behaviour of the different lines in the above figure, taking into account the depth to be investigated ( $< 7$  km), suggests to limit the expansion up to the linear terms and, in this case, the value of  $\alpha_{ss}|_{dB}$  of Eq. 10 can be written as:

$$\begin{aligned} \frac{P_{ss}}{P_s}|_{dB} &= \alpha_{ss}|_{dB} \\ &= \alpha_{00} + k_{ss,R} f_0 z \\ &= \alpha_{00} + k_{ss,\tau} f_0 \Delta\tau \end{aligned} \quad (11)$$

where

$$k_{ss,R} = k_{ss,\tau} \frac{2\sqrt{\varepsilon'_m}}{c} \quad (12)$$

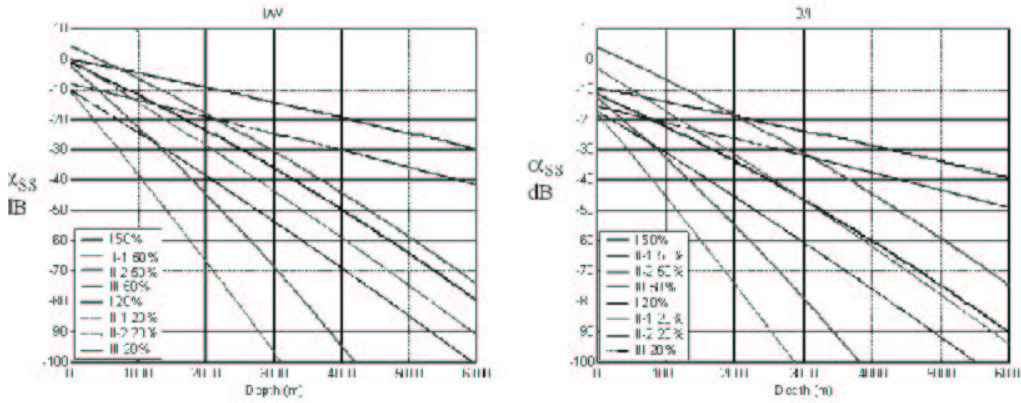


**Fig. 1.** Value of the parameter  $\alpha_{ss}$  in Eq. 10 as a function of depth for different subsurface interface detection scenarios.

in which  $c$  is the speed of light in free space ( $0.3 \text{ km}/\mu\text{s}$ ),  $\overline{\varepsilon'_m}$  is the mean value of the dielectric constant of the mixture in the first layer, and  $z$  is depth in km.

The attenuation of the subsurface interface with reference to the surface value  $\alpha_{ss}|_{dB}$  is composed of a constant term  $\alpha_{00}$  (attenuation at  $z = 0$  depending from the Fresnel reflectivity term  $\Gamma_s(0)$ ) and of one terms proportional to the interface depth (frequency dependent) dependent from the interface reflection coefficient  $R_{12}$  defined by Eq. 7.

#### 4. Approach to MARSIS data inversion

The data inversion is based on the estimation of the following parameters:

- Global reflectivity
- Subsurface attenuation

These parameters are available from MARSIS data and provide a preliminary information regarding the structural composition of the first layer of the Martian surface. If the scattering terms depending on the surface geometric structure are known (through MOLA data) or are the same for the surface and subsurface, we can estimate the first layer dielectric constant: in this way, via the association with the best fit between the available models, we can obtain a preliminary estimation of the first layer composition down to a depth in which we can estimate also the pore filling material.

The inversion problem can be, therefore, related to the estimation of the parameters present in Eq. 11 frame by frame.

The estimation will be obtained along the orbit direction considering the mean value of multiple profiles selected by considering the radar spatial resolution. This procedure, when the orbits are available, should be performed either on parallel orbits as well in perpendicular orbit (on the same area) and with different solar zenith angles. This estimation can be improved if the surface is stationary. Through the parameters present in Eq. 11 it is possible to estimate the dielectric constant of the subsurface material as well the intrusion percentage. The compatibility

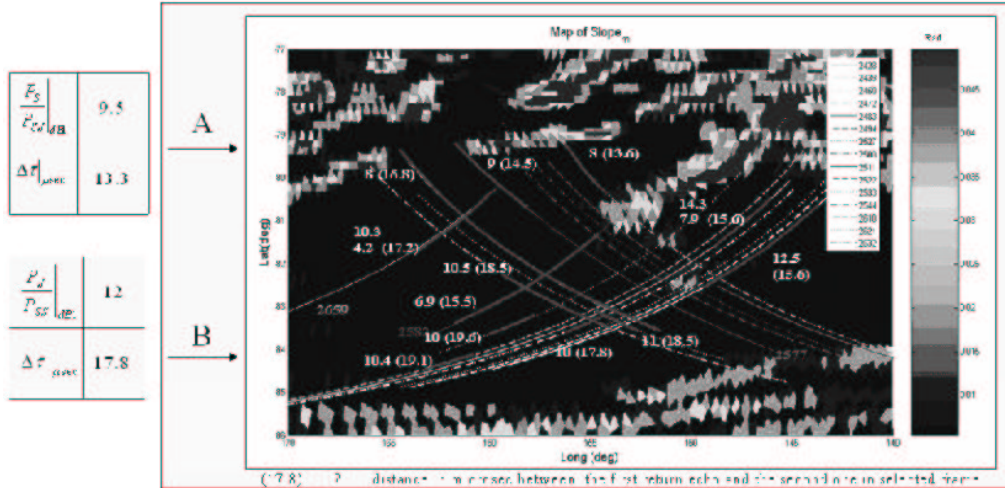


**Fig. 2.** Plot of the ground tracks for two groups of orbits, identified as A and B, over a map of the surface slope  $m$  for an area located in the southern polar terrains of Mars.

with the parameters assumed as a reference model will have an uncertainty due to the relative radar calibration accuracy. The data inversion problem, related to the knowledge of the structural composition of the first layer and of the subsurface discontinuity, is based on the estimation of the attenuation and the time delay between the first surface echo and the subsurface interface. This will be achieved through a best fit approach between the available models and the data obtained from the radar. The accuracy in the knowledge of the permittivity is, obviously, influencing the accuracy on the estimation of the layer thickness.

The inverted data should be analyzed by the geologists in order to select the most appropriate material identification according to the background information and the physical and geological constraints.

The data inversion does not have an unique solution because the number of unknowns is higher than the available equations. Therefore is necessary to make few starting assumptions.

In addition to reduce the number of obtained solutions it is necessary to introduce few constraints relevant to the geological history of the surface, to the local temperature and to all the hypothesis performed on the estimated material on the areas under investigation.

Once a potential signal has been detected, the following verifications must be performed:

- Analysis of the surface backscattering in cross track direction. This analysis is performed also with the help of a simulator (utilizing MOLA data) in order to provide confidence that the surface clutter does not affect the subsurface return echoes.
- Multi frequency analysis in order to estimate the frequency dependent parameters affecting the behavior of the radar echoes.

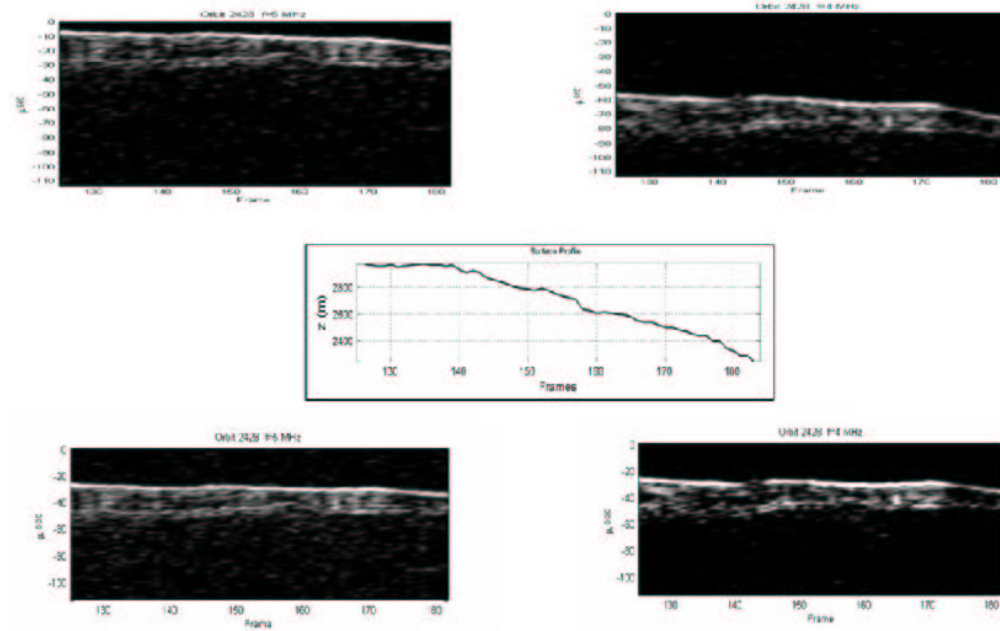


**Fig. 3.** Radargrams for different orbits over the same area, after correction for signal distortion caused by the ionosphere. In the center, a MOLA topographic profile for the same ground track is shown for comparison.

- Analysis of the return echoes from adjacent available orbits to differentiate between surface and subsurface echoes.
- Analysis of return echoes from different regions (supposing same composition of the first layer materials), in order to obtain information of the first layer composition vs. depth. In this case the surface/subsurface hypothesis of stationary is necessary.
- Integration of selected frames, in order to improve the signal to noise ratio.
- Correction of the signal time delay with reference to the range gate due to the altimeter tracking error.
- Correction of ionosphere effects on radar signal by ionosphere plasma frequency estimation.

The parameters estimation (power and time delay) will be obtained along the orbit direction considering the mean value of multiple profiles selected by considering the radar spatial resolution.

The inversion approach is based on the area definition in which the stationary hypothesis is consistent, on the selection of proper areas in which a first layer depth is comparable, and on the selection of proper frames in selected orbits, taking into account the surface and subsurface behavior and the local stationary hypothesis.

The data inversion is based on the estimation of the coefficients  $\alpha_{00}$  and  $k_{ss,R}$  in Eq. 11. The value of  $\alpha_{ss}|_{dB}$  represents the attenuation of the subsurface interface with reference to the surface value. Its value is composed of a constant term and one term, frequency dependent, proportional

**Table 3.** Time delays and power ratios between surface and subsurface echoes for the two groups of orbits shown in Fig. 2. The resulting mean values of  $k_{ss,\tau}$ ,  $\Delta\tau$  and  $k_{ss,\tau} f_0 \Delta\tau$  are respectively 0.185, 12.5 and 9.25 for orbit group A, and 0.139, 17.8 and 9.89 for orbit group B.

Orbit	Lat.	Lon.	Sun elev.	$\Delta\tau$	$f_0 = 5$ MHz	$f_0 = 4$ MHz	$f_0 = 3$ MHz	$h$ (Km)	Frames	$k_{ss,\tau}$
					$P_s/P_{ss}$ ( $P_s/P_v$ )					
2500	-79.3	-156	-4	12.8	11.3 (16)	9.2		351	56-58	0.164
2511	-80.8	-153.6	-3	12.4	14.5 (20)	12		326	99	0.201
2522	-80.9	-154.3	-4	12.9		6.6 (15)	4.1	315	87	0.193
2533	-81.5	-153.6	-4	12.3		6 (25)	3.5	302	94	0.203
2544	-80.4	-158	-6	12.1		5.3 (9)	3.3	301	145	0.165
2610	-81.2	-160.5	-8	17.6		6.2 (20)	3.7	281	130	0.142
2621	-83	-155	-7	17.3		5 (12)	2.5	289	37	0.144
2621	-84	-150	-7	17.7		8 (20)	5.5	292	48	0.141
2626	-82.7	-163.6	-0.1	17.2	12.1 (22)	9.5		359	29	0.151
2632	-83	-156.2	-8	19.5		2.5 (0)	0	295	134	0.128
2632	-82	-159.2	-8	18.3		5.7 (20)	3.4	282	124	0.125
2659	-81.2	-162.2	-1.7	18.3		7.1 (20)	4.5	433	37-39	0.144
2742	-83.3	-166	-13	18.9		9.9 (20)	7.2	450	34-35	0.142

to the interface depth. The available data by the radar echoes, that can be measured (representing estimated values) are the surface power  $P_s$ , the subsurface power of the interface  $P_{ss}$  and the time delay between the first reflection echo and the subsurface interface echo  $\Delta\tau$ . It has to be highlighted that an uncertainty in the knowledge of the permittivity translates into an error on the estimation of the layer thickness ( $\Delta\tau$ ).

## 5. Selection of orbits for data inversion

In order to select the most suitable orbits (e.g. ground track on flat surface) a number of maps has been drawn representing the statistical parameters useful for the surface identification. In Fig. 2 it is shown the map of the slope with superimposed the ground tracks of orbits utilized preliminarily for the data inversion. The orbits have been selected on a region as flat as possible to avoid false subsurface echoes due to clutter.

In Fig. 3 are reported, as an example, typical radargrams relevant to the orbits 2428, 2621, 2632 and 2494 that have been selected because their ground tracks pertain to a smooth surface area of the South polar region of the planet. The processing takes into account the compensation for the gate aperture (tracking gate) and the ionosphere delay considering that the aperture gate is unique for both the utilized frequencies. The comparison of the radargrams with MOLA profiles shows the correct processing performed. In Table 3 are reported all the parameters obtained by the selected frame of the orbits shown in Fig. 2. The values shown in Table 3 are utilized for the inversion process.

## 6. Issues

Between the main surface echo and the first detected interface there are significant amplitude signals, not justified by the Mars surface model, especially in presence of PI/CM model, that are due to particles impurity that give rise to multiple scattering (volume scattering).

The particle scattering cross-section, under the hypothesis of Rayleigh approximation (the particle radius  $r_i$  is much smaller than the wavelength) is expressed by:

$$\begin{aligned}\sigma_i &= 4 \left( \frac{2\pi r_i}{\lambda} \right)^4 |K|^2 \pi r_i^2 \\ &= \frac{\lambda^2}{\pi} \left( \frac{2\pi r_i}{\lambda} \right)^6 |K|^2\end{aligned}\quad (13)$$

where  $K$  in this context is a complex quantity defined in terms the complex index of refraction of the particle relative to the background medium. This leads to

$$K = \frac{\frac{\epsilon_i}{3.15} - 1}{\frac{\epsilon_i}{3.15} + 2}\quad (14)$$

It has to be considered that, according to the distance between the particle and the wavelength utilized, two models can be utilized. One model considers the scattering as incoherent (particles distance higher than the wavelength) while the other model considers the scattering as a coherent one and the particle scattering has to be summed coherently. The procedure and the analysis is the same utilized when evaluating the electromagnetic scattering by the surface. In order to utilize the more suitable model and perform the scattering evaluation some hypotheses are necessary and need to be supported and confirmed by the geologists.

## 7. Conclusions

The MARSIS data inversion has been performed either on North and South Polar area utilizing selected frames at different frequencies, in different regions and during night, when possible to reduce the ionosphere effects. In this paper is shown the data inversion performed considering the orbits shown in Fig. 2 relevant to the Mars South pole. The analysis of the surface backscattering, within the range referred to the nadir position of  $\sqrt{2 h d}$  (with  $h$  = satellite height,  $d$  = height of a potential interface) has been performed taking into account the maps of the slope  $m$  and of the angles  $\alpha_x$  and  $\alpha_y$  (facets method) obtained from 1/128 deg MOLA DEM). In addition potential backscattering surfaces have been evaluated also in along track direction taking into account that the Doppler beam sharpening reduces the unwanted echoes only of a factor equal to a sinc function. The surface echo simulator program has been utilized in order to validate the absence of the clutter backscattering. The simulator, utilizing only the surface characteristics, allows, by comparison, the analysis of the real data in order to make available the required information expected in terms of clutter (within the error bar due to the uncertainty of the surface models).

We wish to remember that the surface simulation, obtained starting from MOLA data, has been utilized also during the planning activity in order to select the MARSIS operative sequence, to optimize the amount of scientific data, taking into account the data rate available and the scientific target to be investigated during the next part of the mission. We can notice that, in order to obtain the final subsurface composition, a deeper investigation is necessary taking into account other constraints as, for instance, the thermal conditions and the estimated geological history and the composition of the area under investigation. An analysis of the volume backscattering has to

be performed for the evaluation of the signal that are within the range between the first surface echo and the detected subsurface.

### References

- Clifford, S. M. 1993, JGR, 98, 10973  
Orosei, R. et al. 2003, JGR, 108, 10.1029/2002JE001883  
Picardi, G. et al. 2004, PSS, 52, 149  
Picardi, G. et al. 2005, Science, 310, 1925  
Porcello, L. J. et al. 1974, Proceedings of the IEEE, 62, 769  
Smith, D. E. et al. 2001, JGR, 106, 23689